DOI 10.5012/bkcs.2010.31.10.2918

Facile Synthesis of Silver Chloride Nanocubes and Their Derivatives

Seungwook Kim, Haegeun Chung, Jong Hwa Kwon,† Ho Gyu Yoon, and Woong Kim*

*Department of Materials Science and Engineering, Korea University, Seoul 136-713, Korea. *E-mail: woongkim@korea.ac.kr*
†Electromagnetic Environment Research Team, Electronics and Telecommunication Research Institute, Daejeon 305-700, Korea
Received July 21, 2010, Accepted August 16, 2010

We demonstrate a facile route to synthesize silver chloride nanocubes and derivative nanomaterials. For the synthesis of silver chloride nanocubes, silver nitrate and hydrochloric acid were used as precursors in ethylene glycol, and poly (vinyl pyrrolidone) as a surfactant. Molar ratio of the two precursors greatly influenced the morphology and composition of the final products. As-synthesized silver chloride nanocubes showed size-dependent optical properties in the visible region of light, which is likely due to a small amount of silver clusters formed on the surface of silver chloride nanocubes. Moreover, we show for the first time that simple reduction of silver chloride nanocubes with different reducing reagents leads to the formation of delicate nanostructures such as cube-shaped silver-nanoparticle aggregates, and silver chloride nanocubes with truncated corners and with silver-nanograin decorated corners. Additionally, we quantitatively investigated for the first time the evolution of silver chloride nanocubes to silver chloride nanocubes decorated with silver nanoparticles upon exposure to e-beam. Our novel and facile synthesis of silver chloride related nanoparticles with delicately controlled morphologies could be an important basis for fabricating efficient photocatalysts and antibacterial materials.

Key Words: AgCl, Nanocubes, Selective etching, Selective reduction, Ag aggregates

Introduction

Silver chloride (AgCl) related materials such as AgCl nanoparticles, silver (Ag) nanograin decorated AgCl nanoparticles, and aggregated Ag nanoparticles have a variety of photochemical and biomedical applications. It is well known that AgCl can be used for the fabrication of photographic paper and photochromic lenses.[1,2] It also has photocatalytic activities that are useful for water splitting and decomposition of organic pollutants.[3-6] It has been demonstrated that decoration of AgCl with Ag nanoparticles can greatly improve the light absorption property and photostability of the AgCl nanoparticles.[7-9] In addition, AgCl can be used in fabricating antiseptic catheters, bone cements, and fabrics owing to its antibacterial property.[10-12] Moreover, aggregated silver nanoparticles can be employed as substrates for surface enhanced Raman spectroscopy (SERS).[13]

Despite the wide range of application of AgCl-related materials, there have been only a few methods available for the synthesis of AgCl nanoparticles such as microemulsion technique or matrix based technique.[3,14,15] Moreover, AgCl nanoparticles with controlled size and shape were produced only under particular conditions. For example, AgCl nanocubes which are surrounded by six (100) facets can be prepared using gelatin matrix.[15] Only very recently, much facile synthesis of AgCl nanocubes without using gelatin matrix has been demonstrated *via* a simple reaction between silver nitrate ($AgNO_3$) and sodium chloride (NaCl) in ethylene glycol.[9] Fine control of the size and shape of the AgCl-related materials may further enhance their catalytic, optical, and electronic properties as demonstrated with various metallic, semiconducting, and metal oxide materials.[16-19] Therefore, it is important to develop facile methods to synthesize size- and shape-controlled AgCl-related nanomaterials.

In this paper, we demonstrate that AgCl nanocubes can be readily synthesized, and that various nanoparticles with delicately controlled morphologies can be derived from the AgCl nanocubes. The AgCl nanocubes can be synthesized by simply mixing two precursors, $AgNO_3$ and hydrochloric acid (HCl) with poly(vinyl pyrrolidone) (PVP) capping agent in ethylene glycol. Depending on the concentration ratio of the two precursors, various final products such as AgCl nanocubes, Ag-grain decorated AgCl nanoparticles, and Ag nanowires can be produced. Size-dependent optical properties of as-synthesized AgCl nanocubes were observed, and they were attributed to small Ag nanoclusters formed on the surface of AgCl nanocubes. Moreover, we demonstrate that simple reductions of AgCl nanocubes with various reducing agents lead to the production of diverse derivatives such as cubic shaped Ag nanoparticle aggregates, AgCl nanocubes with eight corners selectively truncated, and AgCl nanocubes decorated with Ag nanoparticles selectively at eight corners. Additionally, formation of Ag nanoparticles on the AgCl nanocubes under electron beam (e-beam) irradiation was studied. The morphologies, compositions, and structures of the various nanoparticles were characterized by scanning electron microscopy (SEM), energy dispersive X-ray spectroscopy (EDX) and X-ray diffraction (XRD).

Experimental Section

Anhydrous ethylene glycol (99.8%), $AgNO_3$ (99+%), PVP (M.W. ≈ 55,000), HCl (37%), sodium borohydride ($NaBH_4$, 99%), citric acid (CA, 99%), and L-ascorbic acid (LAA, 99%) were purchased from Sigma-Aldrich. Acetone (99.8%) and HNO_3 (60%) were purchased from J.T.Baker and Samchun Chemical, respectively.

AgCl nanocubes were synthesized *via* the reaction of $AgNO_3$ and HCl in ethylene glycol in the presence of a capping agent, PVP. 425 mg of $AgNO_3$ (~ 50 mM) and 415 mg of PVP (~ 75 mM) were dissolved in 50 mL of ethylene glycol. After mixing the solution with a magnetic stirrer for 5 min, a small amount of HCl was added to the solution. Final concentration of HCl was adjusted to the range of 2.5 mM to 300 mM. The solution was then heated to 150 °C. The reaction lasted at this temperature for 20 min unless specified. After the solution was cooled down to room temperature, 100 mL of acetone and 150 mL of de-ionized (DI) water were added and centrifuged at 2000 rpm for 20 min. The resulting precipitates were white powder. This rinsing process was repeated three times. Weight of the AgCl nanocubes was 300 mg, which indicates that 85% of $AgNO_3$ was converted to AgCl nanocubes. For size-selective separation of nanoparticles, spin speed was adjusted in the range of 1000 to 4000 rpm.

To reduce AgCl nanocubes with $NaBH_4$, 0.6 mL of ice-cold 10 mM of $NaBH_4$ was added to 19.4 mL of DI water containing 15 mg of AgCl nanocubes. The color of the solution changed from white to yellow within 5 min. For the reduction of AgCl nanocubes by relatively mild reducing reagents such as CA and LAA, 1 mL of 10 mM reducing reagents was added to 9 mL of DI water containing 15 mg of AgCl nanoparticles. The solution was stirred with a magnetic bar for 30 minutes. The products were collected by centrifugation and re-dispersed in DI water.

Absorption spectra of the nanoparticles dispersed in DI water were measured using a UV-vis spectrophotometer (CARY 50, Varian, USA). Morphologies of nanoparticles were investigated with a field emission scanning electron microscope (FESEM, S-4300, Hitachi, Japan) operated at an acceleration voltage of 15 kV. To minimize any reduction of AgCl into Ag during SEM imaging, the samples were coated with a thin platinum (Pt) layer (12 ~ 18 nm) and imaged only for a short period of time (~ 10 sec). EDX (EX-200, Horiba, Japan) was carried out for composition analysis of nanoparticles at relatively low magnification such as 10,000, and higher magnification was avoided to minimize e-beam exposure to the samples. We have not observed any morphological or compositional change during our SEM and EDX analyses on the Pt coated samples under the above-described conditions. The XRD patterns were obtained using X-ray diffractometer (Rigaku D/MAX 2500V/PC, Japan) with the Cu Kα radiation (λ = 0.154 nm) at a scan rate of 5 degree per minute in the 2θ range from 20 ° to 80 °.

The morphology evolution of AgCl nanocubes upon exposure to e-beam was carried out without any Pt coating in SEM under the following conditions; the emission current, acceleration voltage, working distance, and magnification were 10 μA, 15 kV, 13.5 mm, and 10,000, respectively. SEM images of the AgCl nanocubes were taken after 0, 4, 10, and 18 minutes of exposure.

Results and Discussion

AgCl nanocubes, Ag-nanograin decorated AgCl nanoparticles, and Ag nanowires were synthesized by simply reacting $AgNO_3$ with HCl in ethylene glycol in the presence of a capping agent, PVP. Morphologies of the final products were greatly affected by the molar ratio of $AgNO_3$ and HCl (Figure 1a~f). Uniform nanocubes with an edge length (l) of 516 ± 67 nm (mean ± one standard deviation) were obtained when the $AgNO_3$:HCl ratio was 1:6 (Figure 1a). At the ratio of 1:4, nanocubes with smaller size (l = 342 ± 56 nm) were observed together with small portion of microscale particles as shown in Figure 1b. When the ratio was further reduced to 1:2, the shape of the AgCl nanoparticles was not uniform any longer and various forms with a wide size distribution appeared (Figure 1c). When the ratio of $AgNO_3$:HCl was 1:0.67, where there was excess amount of Ag^+ ions compared to Cl^- ions, AgCl nanoparticles decorated with smaller Ag nanoparticles (AgCl:Ag) were produced (Figure 1d). Inset of Figure 1d clearly shows the morphology of these AgCl:Ag nanoparticles. When the relative amount of HCl was further decreased, Ag nanowires started to appear in addition to the AgCl:Ag nanoparticles (Figure 1e). Eventually, at the ratio of 1:0.05, Ag nanowires were dominantly found (Figure 1f).

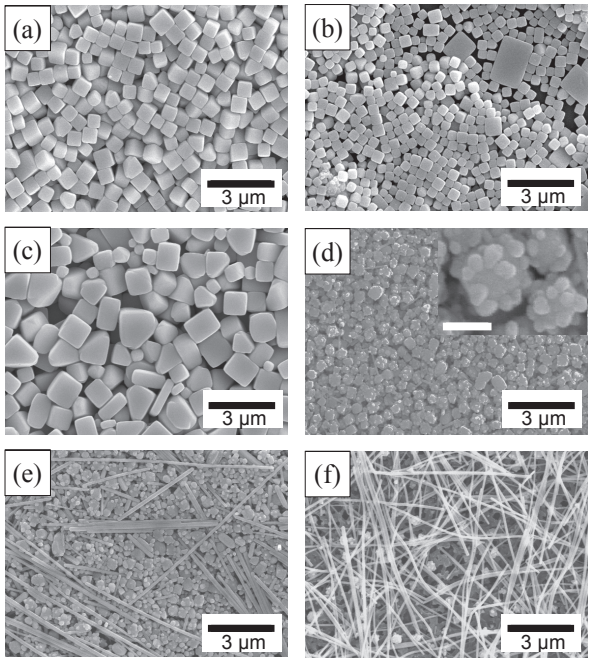

Figure 1. Morphologies of Ag and AgCl based products synthesized with different molar ratio of $AgNO_3$ and HCl; (a) 1:6, (b) 1:4, (c) 1:2, (d) 1:0.67 (inset scale bar = 300 nm), (e) 1:0.33, and (f) 1:0.05.

The composition and the structure of the products were characterized with EDX and XRD. The samples presented in Figure 1a~c showed an atomic ratio of 50:50. This indicates that most of Ag^+ ions reacted with Cl^- ions to form AgCl nanoparticles, and surplus Cl^- ions remained in solution. XRD patterns shown in Figure 2a confirm that these nanoparticles are crystalline AgCl (PDF# 85-1355). When the molar concentration of $AgNO_3$ was greater than that of HCl, atomic Ag:Cl ratio of the nanomaterials also increased accordingly. Atomic ratio of the samples presented in Figure 1d~f was 65:35, 81:19, and 98:2, respectively. This implies that surplus Ag^+ ions were reduced to form Ag nanoparticles or Ag nanowires. AgCl:Ag nanoparticles that correspond to those shown in Figure 1d had both AgCl and Ag peaks in their XRD patterns (Figure 2b). The XRD

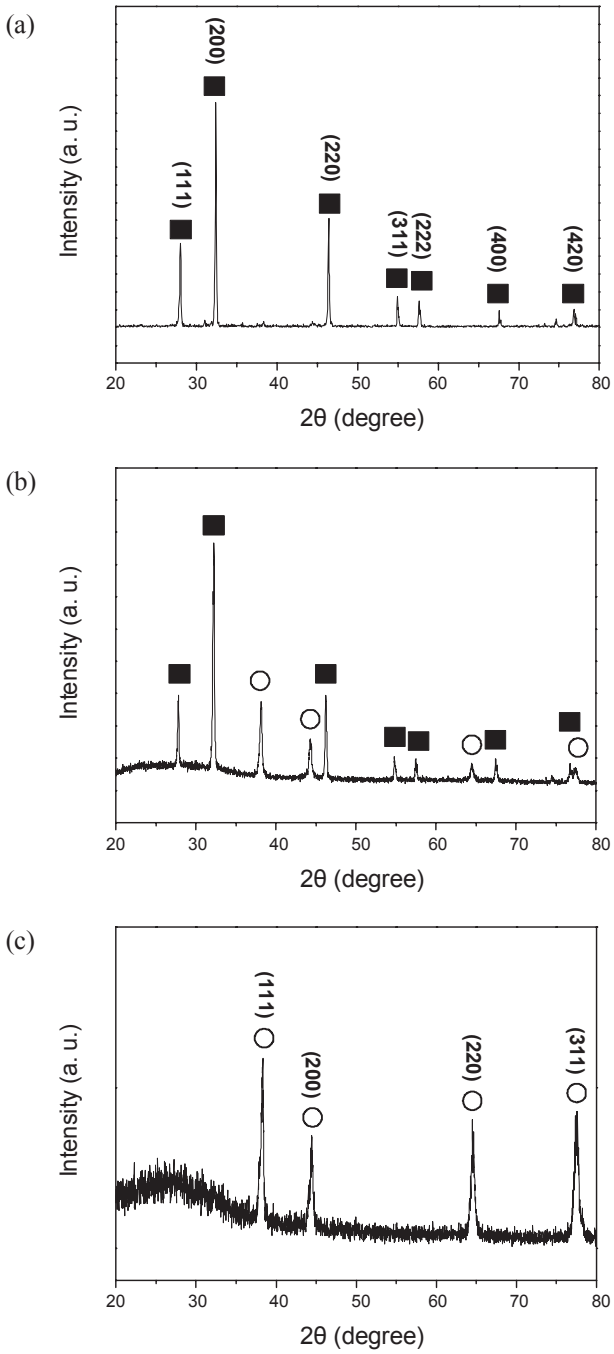

Figure 2. XRD patterns of the samples prepared with $AgNO_3$ and HCl mixed to the ratio of (a) 1:6, (b) 1:0.67, and (c) 1:0.05. Filled square boxes and empty circles indicate XRD peaks of AgCl and Ag, respectively.

patterns of the nanowires shown in Figure 1f match with PDF # 87-0720, which indicates that the nanowires are crystalline Ag (Figure 2c).

To study how precursor molar ratio affects the growth process of AgCl nanocrystals, we observed the change in the morphologies of the nanocrystals over reaction time. The AgCl nanocrystals were collected at two time points; as soon as the solution temperature reached 150 °C (0 min) and after the reaction preceeded for 20 min. At the precursor ratio ($AgNO_3$:HCl)

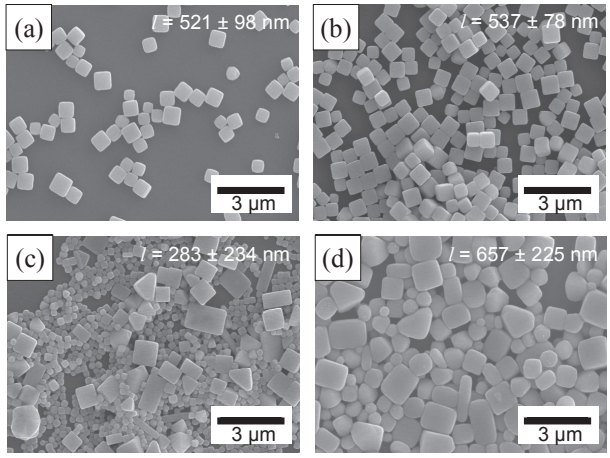

Figure 3. SEM images AgCl nanoparticles produced with the precursor ratio ($AgNO_3$:HCl) of 1:6 at different reaction times; (a) 0 and (b) 20 min. AgCl nanoparticles produced with the ratio of 1:2 at (c) 0 and (d) 20 min. *l* is the edge length or the size of the nanoparticles.

of 1:6, nanoparticles with cubic shape were already formed at 0 min. The cubic shape and size were maintained over time and the size distribution of the nanoparticles became slightly narrower as the reaction proceeded (Figure 3a and b). Edge length of the AgCl nanocubes at 0 and 20 min were 521 ± 98 nm and 537 ± 78 nm, respectively. Narrow size distribution implies that nucleation and growth processes occur homogenously throughout the whole solution. When the precursor ratio was 1:2, Oswald ripening was clearly observed as shown in Figure 3c and d. Edge length of AgCl nanoparticles at 0 min was 283 ± 234 nm. The sample included a number of small nanoparticles with an edge length of 212 ± 48 nm as well as a few percent of large particles. At 20 min, size of the nanoparticles increased in general (l = 657 ± 225 nm), and especially the portion of small nanoparticles was significantly reduced. These results indicate that large nanoparticles grow at the expense of small ones. When the ratio of Ag^+ ions to Cl^- ions is above a certain level, small Ag atom clusters may form locally in the solution and act as nucleation seeds, of which nucleation kinetics could be different from that of silver chloride seeds. Therefore, the presence of different nucleation seeds under high Ag:Cl ratio may explain the wide size distribution of the AgCl particles at the initial stage of growth.

Investigation of optical properties of the AgCl nanocubes showed that as-synthesized AgCl nanocubes absorb light not only in the UV but also in visible region (Figure 4). In addition, the absorption peak in the visible region was red-shifted as the size of nanocubes increased. This visible light absorption may be mainly due to thin Ag clusters formed on the AgCl nanocube surfaces. AgCl has direct and indirect band gap of 5.15 eV (~ 240 nm) and 3.25 eV (~ 380 nm), respectively.[20] Therefore, absorption of light above 380 nm is not possible by AgCl alone. On the other hand, it has been shown that Ag nanoparticles deposited on AgCl show the plasmonic absorption of visible light.[8,9,13] To test our hypothesis that visible light absorption may be due to the Ag atom clusters on the AgCl surface, we treated as-synthesized AgCl nanocubes with HNO_3 (30 wt %)

for 30 min to selectively remove any Ag clusters from the AgCl surface. The absorption profile was significantly modified after the etching process. There was no absorption in the visible region and only strong absorption at $\lambda < 240$ nm was observed, which corresponds to the direct band gap of AgCl (Figure 4f). Our results support the hypothesis that visible light absorption can be attributed to the presence of Ag clusters. On the other hand, size-dependent absorption profile of the AgCl nanocubes is difficult to explain at this point because any close investigation using strong electron or light source instantly changes their composition and morphology by reducing the AgCl into Ag. We conjecture that the size of Ag clusters could be dependent on the size of AgCl nanocubes, and this might have led to size-dependent absorption profile. More detailed experiments and simulations would be necessary to verify this in the future.

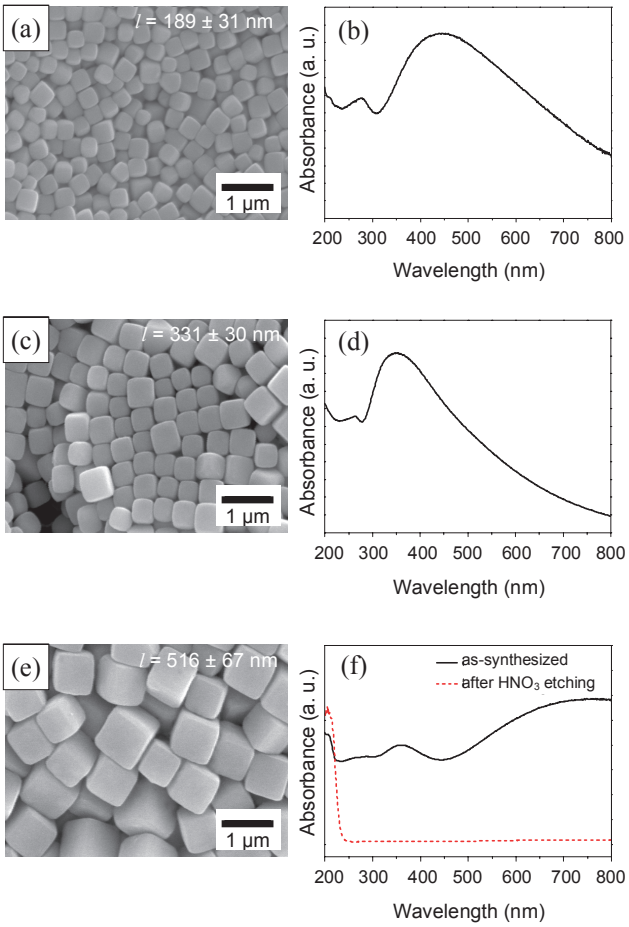

Figure 4. SEM images of AgCl nanocubes with different sizes and their corresponding UV-vis absorption spectra. The edge length of the nanocubes is 189 ± 31 nm for (a) and (b), 331 ± 30 nm for (c) and (d), and 561 ± 67 nm for (e) and (f).

Delicate nanostructures were produced by simply treating the AgCl nanocubes with chemical reagents with different reducing power for the first time (Figure 5). When $NaBH_4$ which is a strong reducing agent was used, the AgCl nanocubes were fully reduced to Ag as confirmed by EDX and XRD analyses. Upon the reduction, the nanocube structure was generally maintained but the formation of small Ag grains in the nanocubes was observed as shown in Figure 5a. These aggregated forms of nanoparticles that have a well-defined shape might be useful for SERS applications. Selective modification of the cubic structure was possible when mild reducing agents such as LAAs and CAs were used. Reduction of AgCl nanocubes with LAAs led to the formation of Ag nanoparticles only at the eight corners of the nanocubes (Figure 5b). When treated with CAs, the AgCl nanocubes were selectively etched. The eight corners of the nanocubes were truncated and small pits were observed dominantly at the corners as shown in Figure 5c. The results indicate that LAAs and CAs can selectively reduce or etch {111} against {100} planes. This can be attributed to the higher surface energy of {111} facets of silver halides compared to that of {100} facets.[21]

Additionally, we directly observed e-beam dependent evolution of AgCl nanocubes into AgCl nanocubes decorated with Ag-nanoparticles for the first time (Figure 6). To study the effect of e-beam exposure on the morphology, the samples were exposed to mild e-beam used for SEM imaging. Emission current (~ 10 μA) and exposed area (~ 120 μm^2) were adjusted so that the reduction process is slow enough for the observation. It should be noted that the samples were not coated with Pt layer in this case unlike other SEM samples shown earlier. Figure 6a~d show the SEM images taken after 0, 4, 10, 18 minutes of exposure time, which correspond to the dose of 0, 20, 50, 90 $\mu C/\mu m^2$, respectively. As the e-beam dose was increased, the number of Ag nanoparticles formed on the AgCl nanocubes increased accordingly. At low dose, the Ag nanoparticles tended to form at the corners and edges of the AgCl nanocubes where the surface energy is higher than that of faces (Figure 6b). At higher doses, Ag nanoparticles were found on the faces of the nanocubes as well (Figure 6c and d). EDX data consistently show that the ratio of silver to chlorine increases over ex-

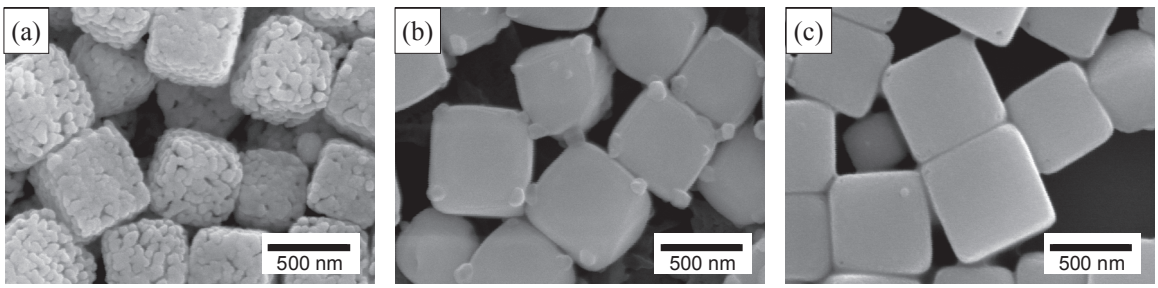

Figure 5. SEM images of (a) cube-shaped Ag-grain aggregates, (b) AgCl nanocubes with Ag nanoparticles at corners, and (c) AgCl nanocubes with truncated corners obtained by reducing AgCl nanocubes with $NaBH_4$, LAA, and CA, respectively.

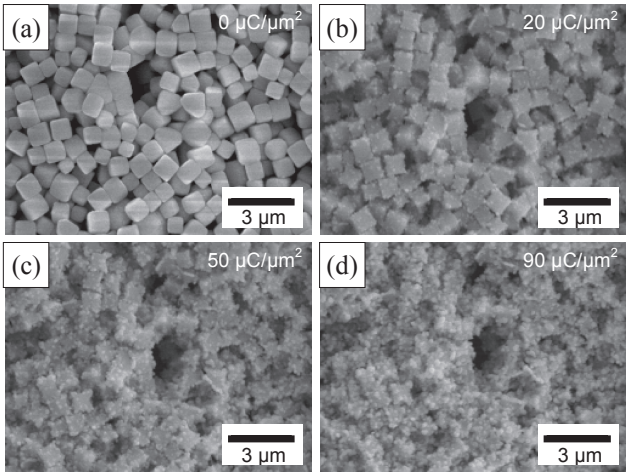

Figure 6. SEM images of AgCl nanocubes exposed to electron beam for various exposure time; (a) 0, (b) 4, (c) 10, and (d) 18 min. Each corresponds to a dose of 0, 20, 50, 90 μC/μm^2, respectively.

posure time; the initial ratio of 51:49 becomes 54:45, 63:37, and 75:25 after 4, 10, 18 min of exposure, respectively.

Conclusions

We have demonstrated a facile synthesis of AgCl nanocubes and their derivatives. AgCl nanocubes were prepared by the reaction between $AgNO_3$ and HCl as precursors in ethylene glycol at 150 ^oC with PVP capping agent. A plasmonic photocatalyst AgCl:Ag were produced in three different ways; 1) by optimizing precursor concentration ratio, 2) by reducing AgCl nanocubes with LAAs, and 3) e-beam exposure. Especially, the LAA treatment led to the formation of Ag nanoparticles selectively at eight corners of the AgCl nanocubes. Cube-shaped Ag nanoparticle aggregates were produced by reducing AgCl nanocubes with a strong reducing agent, $NaBH_4$. Our AgCl-based nanoparticles with delicately controlled morphologies may play an important role in various applications such as photocatalyst, SERS, and antiseptic biomedical devices.

Acknowledgments. This work was supported by the Korea Research Foundation (KRF-2008-331-D00254), the Pioneer Research Center Program through the National Research Foundation of Korea (No. 2010-0002191), and the IT R&D program of MKE/KCC/KEIT (KI001685).

References

1. Hamilton, J. F. *Adv. Phys.* **1988**, *37*, 359.
2. Araujo, R. J. *Contemp. Phys.* **1980**, *21*, 77.
3. Reddy, V. R.; Currao, A.; Calzaferri, G. *J. Mater. Chem.* **2007**, *17*, 3603.
4. Currao, A.; Reddy, V. R.; van Veen, M. K.; Schropp, R. E. I.; Calzaferri, G. *Photochem. Photobiol. Sci.* **2004**, *3*, 1017.
5. Schurch, D.; Currao, A.; Sarkar, S.; Hodes, G.; Calzaferri, G. *J. Phys. Chem. B* **2002**, *106*, 12764.
6. Lanz, M.; Schurch, D.; Calzaferri, G. *J. Photochem. Photobiol., A* **1999**, *120*, 105.
7. Wang, P.; Huang, B. B.; Qin, X. Y.; Zhang, X. Y.; Dai, Y.; Wei, J. Y.; Whangbo, M. H. *Angew. Chem. Int. Ed.* **2008**, *47*, 7931.
8. Choi, M.; Shin, K. H.; Jang, J. *J. Colloid Interface Sci.* **2010**, *341*, 83.
9. An, C. H.; Peng, S.; Sun, Y. G. *Adv. Mater.* **2010**, *22*, 2570.
10. Potiyaraj, P.; Kumlangdudsana, P.; Dubas, S. T. *Mater. Lett.* **2007**, *61*, 2464.
11. Li, C. H.; Zhang, X. P.; Whitbourne, R. *J. Biomater. Appl.* **1999**, *13*, 206.
12. Spadaro, J. A.; Webster, D. A.; Becker, R. O. *Clin. Orthop. Relat. Res.* **1979**, 266.
13. Sun, L. L.; Song, Y. H.; Wang, L.; Guo, C. L.; Sun, Y. J.; Liu, Z. L.; Li, Z. *J. Phys. Chem. C* **2008**, *112*, 1415.
14. Bagwe, R. P.; Khilar K. C. *Langmuir* **1997**, *13*, 6432.
15. Sugimoto, T.; Miyake, K. *J. Colloid Interface Sci.* **1990**, *140*, 335.
16. Lim, B.; Jiang, M. J.; Tao, J.; Camargo, P. H. C.; Zhu, Y. M.; Xia, Y. N. *Adv. Funct. Mater.* **2009**, *19*, 189.
17. Sun, Y. G.; Xia, Y. N. *Science* **2002**, *298*, 2176.
18. Jun, Y. W.; Choi, J. S.; Cheon, J. *Angew. Chem. Int. Ed.* **2006**, *45*, 3414.
19. Tao, A. R.; Habas, S.; Yang, P. D. *Small* **2008**, *4*, 310.
20. Glaus, S.; Calzaferri, G. *Photochem. Photobiol. Sci.* **2003**, *2*, 398.
21. Sugimoto, T. *Monodispersed Particles*; Elsevier Science: Amsterdam, 2001.